G^* = collection of terms defined by Equation (24)
g = acceleration of gravity
H^* = collection of terms defined by Equation (25)
L^* = dimensionless radius ratio = $R_i/(R_o - R_i)$
m_s = mass of sphere
N_{Re} = Reynolds No. = $D_s^2\Omega_i\rho_1/\mu$
$\mathbf{n}$ = unit vector normal to surface of sphere
$\mathbf{q}_1$ = velocity field reflected from inner wall
$\mathbf{q}_2$ = velocity field reflected from outer wall
r = radial coordinate of cylindrical coordinate system associated with Couette system
r_s = radial coordinate of sphere in cylindrical coordinate system
r_s^1 = radial coordinate of spherical coordinate system with origin at center of sphere
R_i = radius of inner Couette cylinder
R_o = radius of outer Couette cylinder
R^* = $(r - R_i)/R_o - R_i)$ = dimensionless radial position
t = time
T^* = $t\Omega_i$ = dimensionless time
$\mathbf{u}$ = fluid velocity
u_t = tangential velocity of fluid in Couette system
$\mathbf{u}_{fs}$ = free stream velocity
$\mathbf{v}$ = velocity of center of sphere
v_r = velocity of sphere in $\mathbf{e}_r$ direction
v_t = velocity of sphere in $\mathbf{e}_t$ direction
V^* = $v/(R_i\Omega_i)$ = dimensionless velocity
W^* = $w/(R_i\Omega_i)$ = dimensionless lag velocity
w = lag velocity
x, y, z = Cartesian coordinates with origin at center of sphere
z_s = vertical coordinate of sphere in Couette region

Greek Letters

$\mathfrak{S}$ = stress tensor
κ = gradient in free stream velocity
μ = viscosity
ρ_s = density of sphere
ρ_1 = density of liquid
ρ^* = reduced density difference = $(\rho_1 - \rho_s)/\rho_s$
τ = ratio sphere diameter to annular thickness of Couette region = $D_s/(R_o - R_i)$
ω_s = tangential velocity of sphere surface due to rotation about its own axis
Ω_s = angular speed of rotation of sphere about its own center
Ω_i = angular speed of rotation of inner Couette cylinder

LITERATURE CITED

1. Segré G., and A. Silberberg, *Nature*, **189**, 209-210 (1961).
2. Oliver, D. R., *ibid.*, **194**, 1269-1271 (1962).
3. Denson, C. D., Ph.D. thesis, Univ. Utah, Salt Lake City (1965).
4. Jeffrey, R. C., and J. R. A. Pearson, *J. Fluid Mech.*, **22**, 721-735 (1964).
5. Theodore, Louis, Sc.D. dissertation, N. Y. Univ., New York (1964).
6. Rubinow, S. L., and J. B. Keller, *J. Fluid Mech.*, **11**, 447-459 (1961).
7. Brenner, Howard, in "Advances in Chemical Engineering," T. B. Drew et al. ed., Vol. 6, p. 399, Academic Press, New York (1966).
8. Saffman, P. G., *J. Fluid Mech.*, **22**, 385-400 (1965).
9. Harper, E. Y., and I-Dee Chang, *ibid.*, in press.
10. Halow, J. S., and G. B. Wills, Va. Acad. Sci., Eng. Div. (1967).
11. Halow, J. S., Ph.D. thesis, Va. Polytechnic Inst., Blacksburg (1967).
12. Oseen, C. W., "Neue Methoden und Ergebnisse in der Hydrodynamik," p. 114, Akademische Verlagsgesellschaft, Leipzig (1927).
13. Lorentz, H. A., *Versl. K. Akad. W. (Amsterdam)*, **5**, 168 (1897); "Collected Papers," 1 ed., Vol. 4, pp. 7-14, Martinus Nijhoff, The Hague (1937).
14. Lamb, Sir Horace, "Hydrodynamics," 6 ed., pp. 594-597, Cambridge University Press, Cambridge, England (1932).
15. Wakiya, Shoichi, *J. Phy. Soc. (Japan)*, **12**, No. 10, 1130 (1957).
16. Faxen, O. H., *Arkiv. Mat. Astron. Fys.*, **17**, No. 27 (1923); dissertation, Uppsala Univ., Sweden (1921).

Manuscript received October 26, 1967; revision received September 12, 1968; paper accepted September 16, 1968.

Absorption and Scattering of Thermal Radiation by a Cloud of Small Particles

A. R. NAGY, JR., and J. M. LENOIR

University of Southern California, Los Angeles, California

An experimental investigation was made of the absorption and scattering of thermal radiation by a cloud of small, spherical, micronsized, aluminum oxide particles in a plane-parallel enclosure. By using carbon tetrachloride and carbon disulphide as suspending media, transmission measurements were made with collimated and diffuse sources for wavelengths from 2 to 11μ. By employing a two-flux diffuse model, the data were correlated to obtain absorption and backscattering cross sections. From the diffuse and collimated data, a backscatttering coefficient was found which varied linearly with relative refractive index. With the developed coefficients, the absorptivities of the cloud of particles were determined.

For clouds of small particles with diameters of 10μ magnitude, the prediction of heat transfer rates by radiant transfer to and from the particles is not only mathematically complex but also subject to uncertainties caused by nonspherical shape, size distribution, and nonuniform

A. R. Nagy, Jr. is with the Aerospace Corporation, El Segundo, California.

composition. With high particle density, multiple scattering exists along with absorption. Such situations where ability to predict radiant transfer becomes important exist with pneumatic flow, or with fluidized beds, at high temperature, sometimes in furnaces, and also in the plume of a rocket exhaust containing metal oxide particles. It is the purpose of this investigation to indicate a way to measure the transmission characteristics of various cloud concentrations and from the optical properties obtain a method for predicting the effective absorptivity of the cloud by using an infrared spectrophotometer. Although at present this procedure has been used only for solid particles suspended in fluids at 25°C., the potential is believed to exist for extension to other conditions.

THEORETICAL MODEL

The formulations of the equation of transfer which precisely describes conservation of radiant energy are numerous (*1* to *4*) and will not be repeated here. Since they are generally nonlinear, integro-differential equations, solutions have been obtained for only very restricted cases. The work of Love (*4*) is an example of this, in which a transfer equation was solved by the method of discrete ordinates for particles with a specific index of refraction.

Morizumi and Carpenter (*5*) approached the problem of describing the thermal radiation from the exhaust plume of a solid propellant rocket motor by using a model analogous to isotropic neutron scattering. Stull and Plass (*6*) computed the absorption and scattering cross sections of small carbon particles from the Mie theory (*7*). From a simplified equation of transfer they (*6*) were able to compute the emissivity of a dispersed cloud by a finite-difference approach using a coarse mesh for calculations. The scattered energy was small in this case. McAlister et al. (*8*) performed an analysis and experiment to obtain the absorptivities of a cloud of particles using zinc, ferrous sulfide, and cupric oxide without considering the contribution made by scattering.

All of the above works were idealized; that is, scattering was small, isotropic, or neglected, or the results were too complex to be used with experimental correlations. In order to place the results of the present investigation in more tractable form, a two-flux model which essentially divides a diffuse radiation field into two fluxes, one forward and one backward, was considered. This was first suggested by Schuster (*9*), Kubelka and Munk (*10*), and utilized by Hamaker (*11*). More recently, Larkin and Churchill (*12*) have successfully used it to correlate radiation through porous insulative materials, and Chen and Churchill (*13*) have used it for packed beds. Lathrop (*14*) emphasized that the radiant flux must be diffuse in order for the two-flux assumption to apply. Churchill, Clark, and Sliepcevich (*15*), when investigating scattering effects in dispersions of latex particles, determined that a correction for net side-by-side loss of radiation in the two-flux model was very small.

The two-flux model used to correlate the experimental results was similar to those developed in the above-mentioned works with the following exceptions.

1. Emission was neglected.
2. Absorption of the suspending media was included.
3. Reflectivity of the cell windows was considered.
4. Rereflections, being of minor importance, were neglected.

The following differential equations described the energy balance on both the forward and backward fluxes. For the forward

$$\frac{di}{dx} = -inB\sigma_s - in\sigma_a - i\alpha_m + jnB\sigma_s \qquad (1)$$

The first three terms on the right-hand side of Equation (1) represent the loss in intensity due to the backscattering by the particles, absorption by the particles, and absorption by the suspending medium. The last term represents a gain in intensity by the backscattering of the backward flux. The backward flux shows a similar balance:

$$\frac{dj}{dx} = jnB\sigma_s + jn\sigma_a + j\alpha_m - inB\sigma_s \qquad (2)$$

These equations can be combined to obtain the following uncoupled equations:

$$\frac{d^2i}{dx^2} = (a^2 + 2ab)\, in^2 \qquad (3)$$

$$\frac{d^2j}{dx^2} = (a^2 + 2ab)\, jn^2 \qquad (4)$$

where

$$a = \sigma_a + \alpha_m/n$$

$$b = B(\sigma_e - \sigma_a) = B\sigma_s$$

The boundary conditions at the edges of the cloud are

$$x = 0 \qquad i = i_0$$
$$x = L \qquad j = \rho i$$

Equation (3) can be solved to obtain

$$\frac{i(L)}{i_0} = 1 \Big/ \left\{ \cosh(mnL) + \left[\frac{a + b\,(1-\rho)}{m}\right] \sinh\,(mnL) \right\} \qquad (5)$$

Normalizing Equation (5) with respect to the transmissivity of the suspending medium we get

$$T = \exp(\alpha_m L) \Big/ \left\{ \cosh(mnL) + \left[\frac{a + b\,(1-\rho)}{m}\right] \sinh(mnL) \right\} \qquad (6)$$

The details of the derivation were carried out by Nagy (*16*). With this model and sufficient experimental data, the empirical constants a and b can be obtained to predict the absorptivity of the cloud from

$$\alpha = 1 - r - T$$

The expression for the absorptivity for $\rho = 0$ becomes (*16*)

$$\alpha = 1 - [m + b\sinh(mnL)]/[m\cosh(mnL) + (a + b)\sinh(mnL)] \qquad (7)$$

EXPERIMENTAL PROCEDURE

The experimental procedure required three tasks: the separation of particles into uniformly sized batches, the measurement of the size distributions of these batches, and the preparation and measurement of transmission of particle clouds with varying population densities.

The particles selected were spherical aluminum oxide. These materials were selected because they would both absorb and scatter light for the near infrared wavelengths. The initial size distribution for the material ranged below 25μ for the aluminum oxide. They were separated into narrow size ranges by air

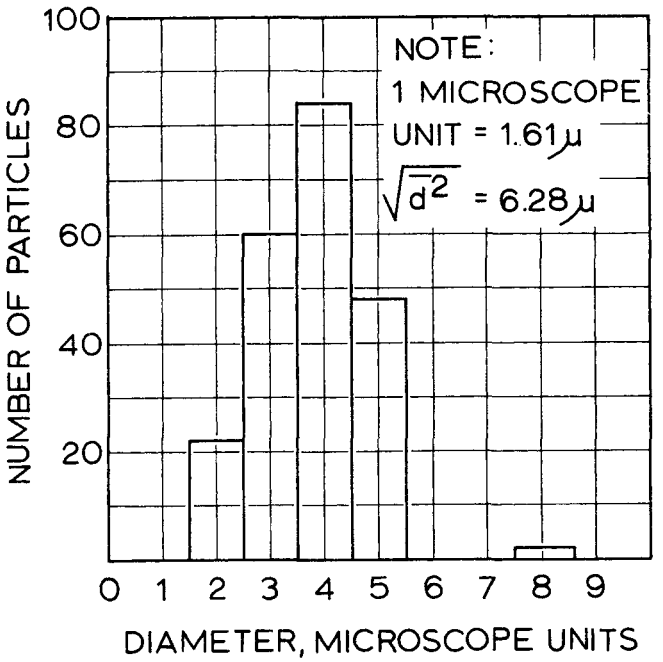

Fig. 1. Measured size distribution for aluminum oxide, 5- to 7.5-μ cut.

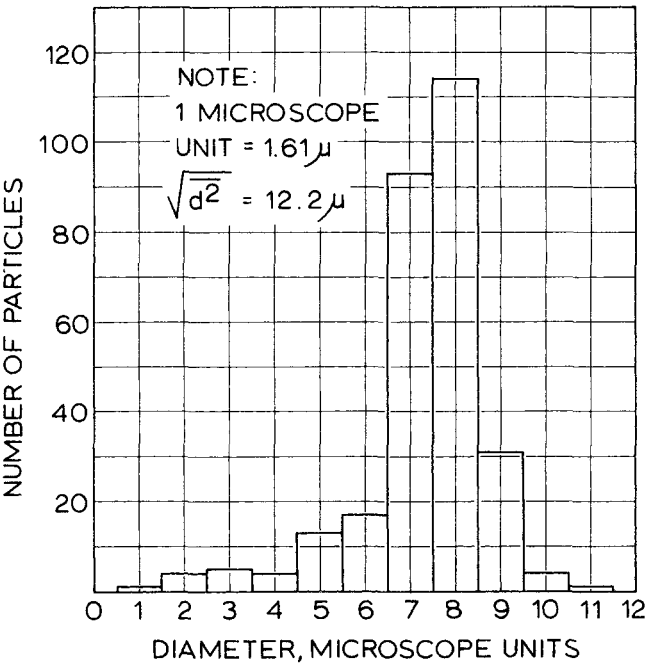

Fig. 2. Measured size distribution for aluminum oxide, 10- to 12.5μ cut.

elutriation by using a silver lined glass settling chamber 6 in. in diameter and 48 in. high. The size distribution of each range was determined by use of an optical microscope. Although the particles appeared to be perfect spheres, about one in twenty were entirely irregular in shape.

The particle clouds were prepared by placing a weighed sample of the aluminum oxide into suspension with either of the selected media, carbon tetrachloride or carbon disulfide. The suspension was transferred to the cell, which was the shape of a right circular cylinder, made of polished stainless steel, 2.39 cm. in diameter and 1.43 cm. in length. Servofrax (arsenic trisulfide) windows were used at the ends of the cylinder to contain the suspension. This material was selected because it was a glass, was nonhygroscopic, and was easy to handle. Flat circular seals made of Viton A were used between the windows and the ends of the cylinder.

The transmission measurements made for both collimated and diffuse sources were in the range of wavelengths from 2 to 11μ by using a Beckman 1R 2-A spectrometer. The instrument, as modified, contained four compartments.

1. A light source section with a Nernst glower (a hollow ceramic tube ⅜ in. long and ⅛ in. diameter), a chopper, a mirror, and a collimating lens.
2. A sample section, with a slot for the sample cell and a converging lens to collect the transmitted light.
3. A monocrometer consisting of entrance and exit slits, a light dispersing prism, associated mirrors, and a thermocouple detector.
4. Electronic equipment for amplifying the output signal and converting it to direct current for potentiometer readings.

When the collimated measurements were made, the slits in the monochrometer were set between 0.01 to 0.1 mm., giving a maximum subtended angle of about 2 min. for the slit. Moreover, by applying the diffraction theory of Gumprecht and Sliepcevich (*17*), the solid angle subtended by the monochrometer located within the spectrometer was found to be small enough to essentially eliminate the contribution of forward scattering when measuring the transmission of the collimated source. For the diffuse measurements, the window was roughened with a No. 80 grit paper. The transmitted light through the window was checked on an optical bench and was found to be diffuse.

EXPERIMENTAL DATA

Figures 1 and 2 indicate the size distributions obtained from the separated batches of particles. The aluminum oxide batches had root-mean-square diameters that fell within the range expected from Stokes settling law.

The transmission results obtained from the infrared spectrometer were plotted on semilog coordinate paper. Typical results are shown in Figures 3 and 4. In all cases, the plots of transmission against particle population density for the collimated source fell along a straight line that could easily be drawn through the data. The

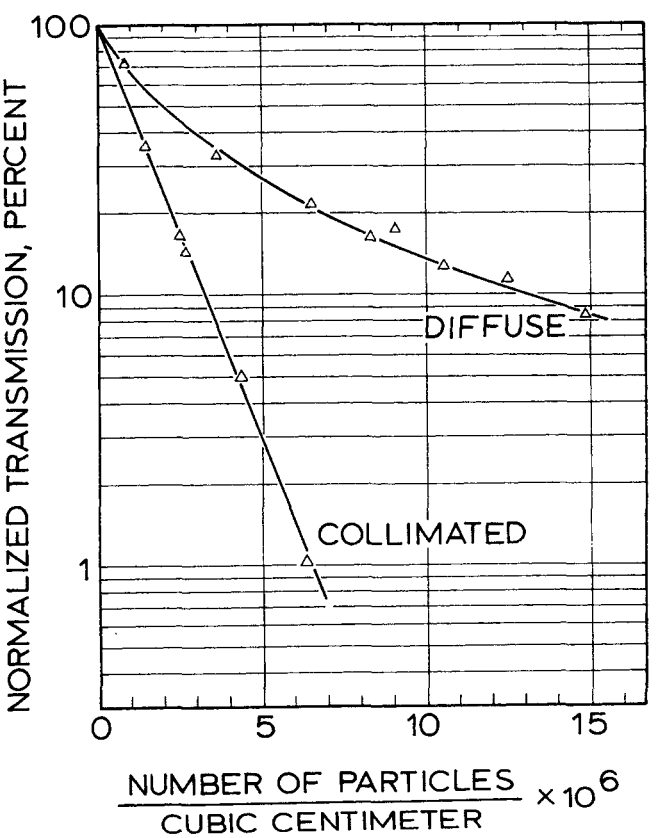

Fig. 3. Transmissivity of aluminum oxide particles in carbon tetrachloride, $d = 6.28\mu$, $\lambda_0 = 4.5\mu$.

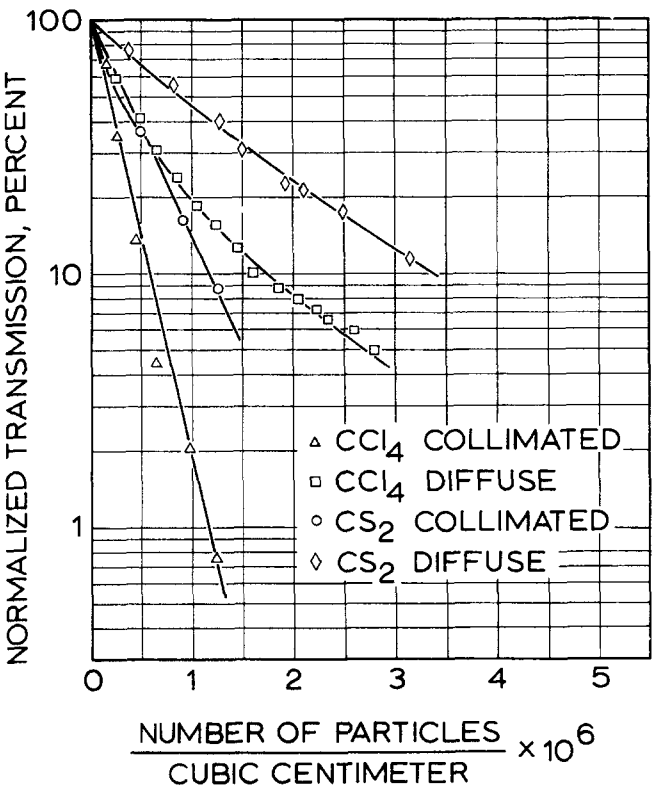

Fig. 4. Transmissivity of aluminum oxide particles, $d = 12.2\mu$, $\lambda_0 = 4.5\mu$.

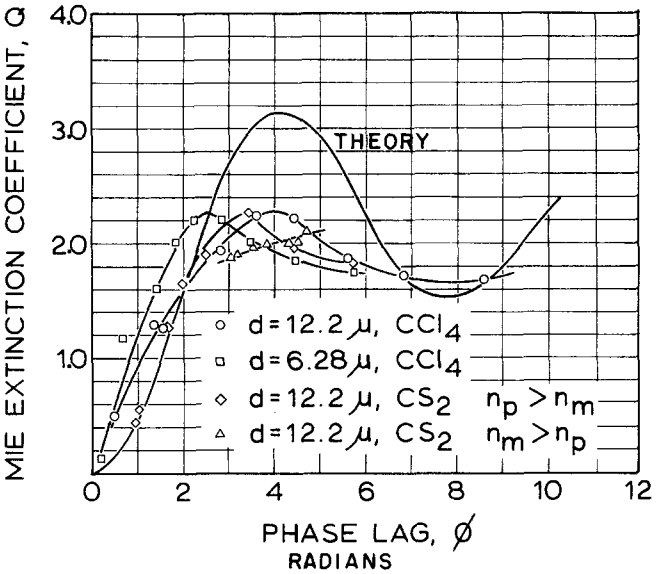

Fig. 5. Mie extinction coefficient for aluminum oxide particles.

Mie extinction coefficients for each diameter and wavelength were obtained from the following equation:

$$Q_e = \frac{-\ln T}{n}\,(4/\pi d^2 L)$$

The straight line plot of the data was consistent with the fact that the extinction coefficient is independent of particle concentration. The extinction cross section σ_e was obtained from $\sigma_e = Q_e \frac{\pi d^2}{4}$. The results for the diffuse source were not linear on the semilog coordinate paper; however, the general shape of the curves was typical for a multiple scattering suspension.

CORRELATION OF RESULTS

The Mie extinction coefficients for the collimated tests were correlated by the phase lag method of Van de Hulst (*18*). The phase lag in radians is equal to $2\pi/\lambda_0$ times the optical path difference between a light ray which passes through the spherical particle along the diameter and one parallel to it in the suspending medium. The phase lag can be represented by

$$\phi = 2\pi d/\lambda_0\ |n_p - n_m|$$

When the two rays are in phase, there will be an increase in intensity and a decrease in the Mie coefficient, while if they are out of phase the opposite is true.

Figure 5 shows the variation of the extinction coefficient for aluminum oxide as a function of the phase lag. The curves drawn through the experimental data indicate that the extrema are somewhat diffused. However, there is reasonable agreement between the maxima of the three sets of data. The variation of the phase lags for maximum extinction could be attributed to the uncertainty in the value of refractive index, since the difference between the indexes of the particles and suspending media was less than 0.3. It is to be expected that the maxima did not match the theoretical Mie values because:

1. The powder, while more monodisperse after being elutriated, still had a finite size distribution. This would tend to diffuse the extrema.

2. The powder was found to be highly crystalline and to include two forms, α and γ, with the latter being the major form. Since these two forms are known to vary slightly in refractive index, the sharpness of the interference patterns that created the extrema would be diffused.

The results plotted for the diffuse transmission were curved in contrast to the linear character of the collimated data. This is characteristic of multiple scattering. Equation (6) was fitted to the data by applying a method of nonlinear least squares described elsewhere (*16*). A good fit was obtained for nearly all of the wavelengths, particle sizes, and suspending media considered. However, as the particle density increased, the scatter of data tended to increase. This was primarily due to the low transmission through the cell and to the reduction of the signal-to-noise ratio of the spectrometer.

For each of the curve fits, values of b and a or B and σ_a were obtained for various diameters and wavelengths. The values of B are given in Figure 6. It can be seen that the values of B for the carbon disulfide suspension are lower than those for carbon tetrachloride. However, when B is plotted against $|n_p/n_m - 1|$ in Figure 7, a general trend was observed. B appeared to vary in a somewhat linear fashion with $|n_p/n_m - 1|$ over the range of test conditions. This general trend is in agreement with the diffraction theory of light which would predict more backscatter by the bending of light rays as the relative refractive index increased. The maximum value of the backscattering coefficient (~ 1) was comparable to that obtained by Roessler and Horlacher (*19*) in their study with a powder of magnesium oxide deposited on a glass slide.

The experimental absorption coefficient, defined as $4\sigma_a/\pi d^2$, is shown in Figure 8. The data representing the absorption coefficient for the larger particle size in the two different media agreed well for the short wavelengths. Although the general trends were consistent for the longer wavelengths, some discrepancy was evident.

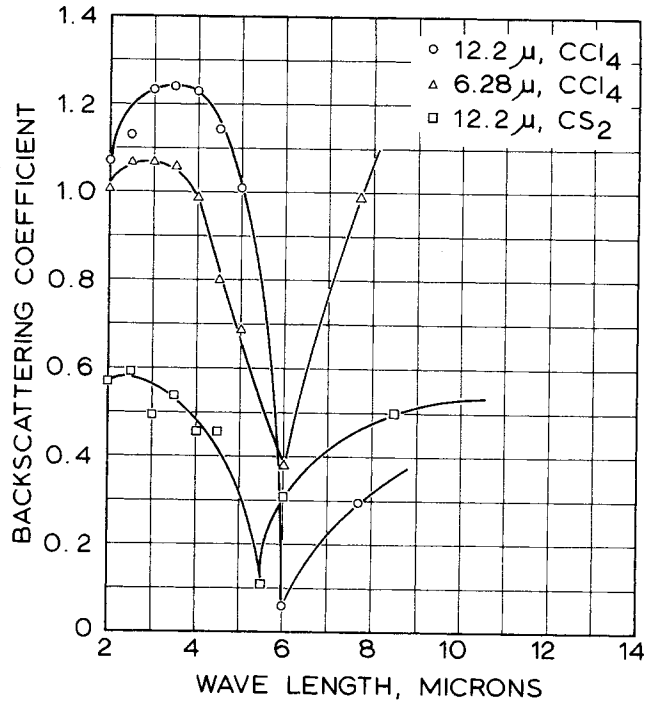

Fig. 6. Backscattering coefficient for various wavelengths.

This discrepancy may have resulted because the higher absorption in these wavelengths altered the diffuse nature of the radiation field. The comparison of the data for 12.2-μ particles with the 6.28-μ particles was in good qualitative agreement. However, the comparison with published data on sapphire indicated the absorption to be higher in the present study. Gillespie et al. (*20*) found the absorption coefficient to be 4.6×10^{-3} by

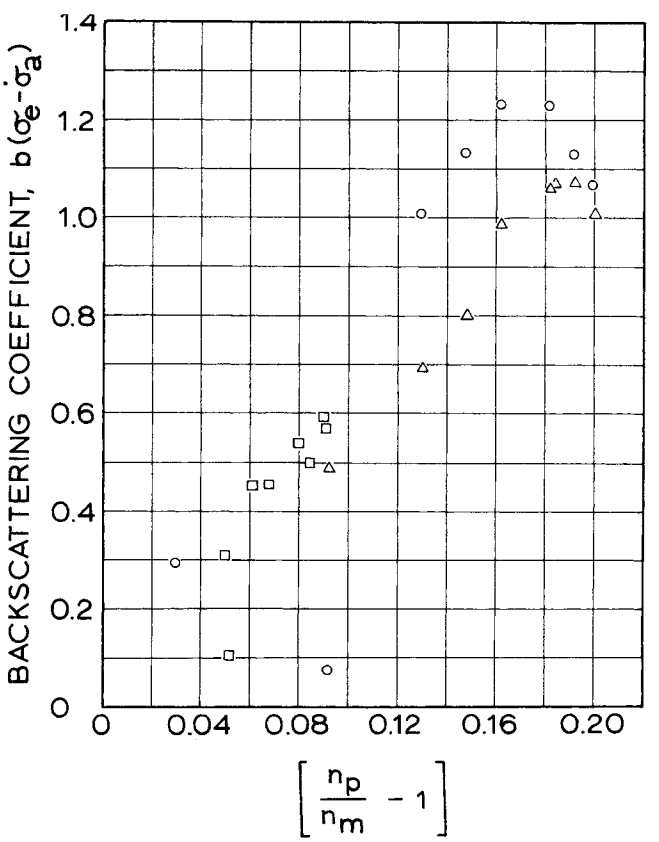

Fig. 7. Backscattering correlation.

measurements made through a piece of sapphire 2.8 mm. thick. The work of McCarthy (*21*) agreed qualitatively with these data. However, earlier work by McCarthy (*22*) indicated a strong absorption band at 2.7μ, claimed to be due to the impurities in the sample of sapphire. Plass (*23*) used the absorption data of sapphire from Gryvnak and Burch (*24*) to compute absorption coefficients from 7×10^{-5} for a wavelength of 2μ to 5×10^{-2} for 6μ. However, emissivity data (*24*) of polycrystalline alumina were observed to be greater than for single crystal sapphire.

Carlson et al. (*25*) measured the emissivity of a rocket plume with aluminum oxide in the liquid state and found it to be two orders of magnitude greater than predicted from data of sapphire in the solid state (*24*). This was probably due to the higher mobility of electrons in the liquid state.

A comparison of the absorption between a disk of polycrystalline magnesium oxide and a single crystal by Hanna (*26*) indicated that the former material had a higher absorption owing to impurities entrapped at the grain boundaries. Lee and Kingery (*27*) found this same effect. Florio (*28*) measured the dielectric properties of the single crystal and polycrystalline aluminum oxide and found the electrical conductivity for the latter to be higher by two orders of magnitude. The former was found to be 99.99% pure, while the latter had impurities of 0.5% consisting of iron, silicon, sodium, magnesium, and calcium. From electromagnetic theory (*29*), the Mie absorption cross section was shown to be proportional to the electrical conductivity. This fact suggested that the relatively impure polycrystalline phase would have a higher absorption cross section. Morizumi and Carpenter (*5*) concluded that the data of sapphire were not representative of the aluminum oxide particles in rocket exhausts.

Thus, polycrystalline aluminum oxide is not optically identical to sapphire. The higher absorption coefficients obtained in the present work were not inconsistent with those obtained in other investigations dealing with the polycrystalline phase.

APPLICATION OF RESULTS

Once the values of σ_a, σ_e, and B are determined, it is

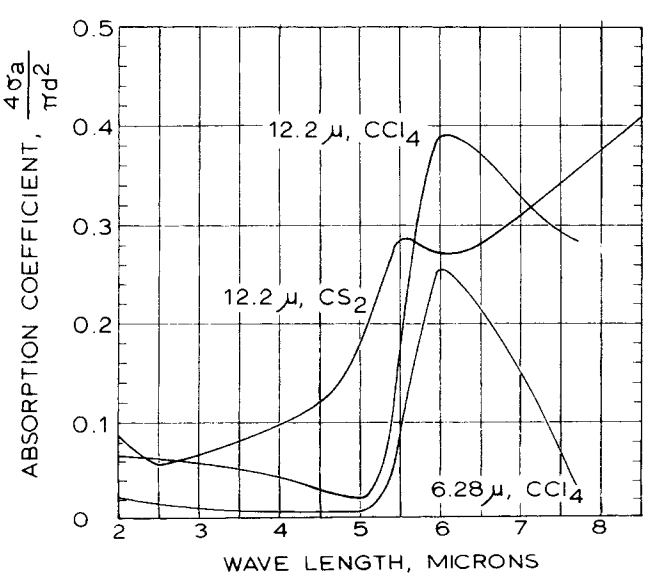

Fig. 8. Absorption coefficient of aluminum oxide particles.

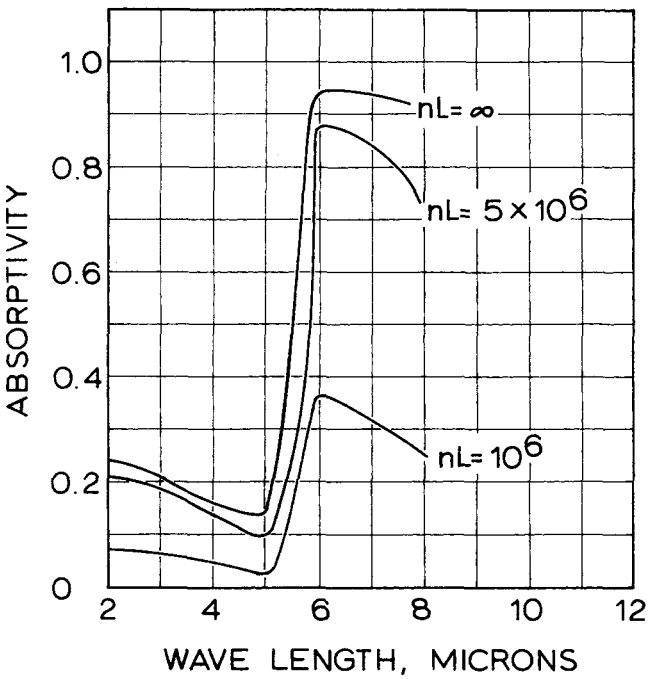

Fig. 9. Absorptivity of a cloud of aluminum oxide particles with a diameter of 12.2μ in carbon tetrachloride.

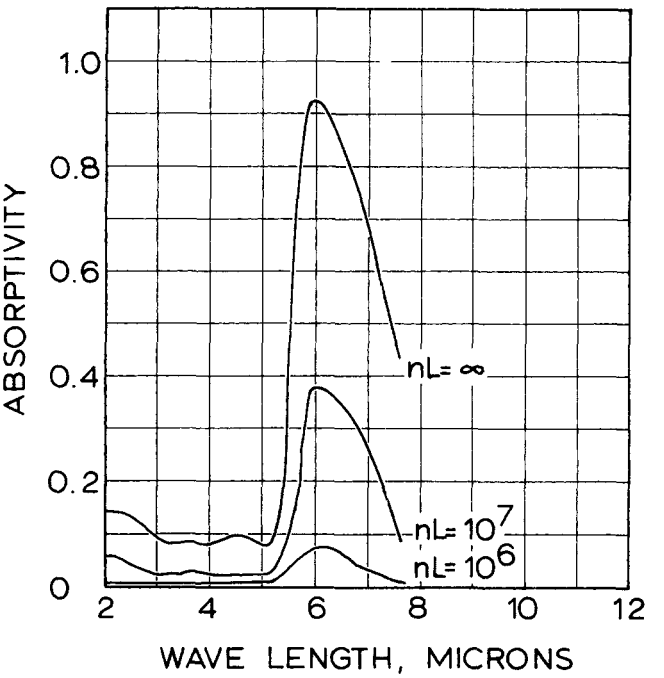

Fig. 10. Asorptivity of a cloud of aluminum oxide particles with a diameter of 6.28μ in carbon tetrachloride.

possible to predict the absorptivity of a plane parallel atmosphere from Equation (7). If the cloud becomes very dense, then, in the limit, Equation (7) becomes

$$\alpha = 1 - b/[(a^2 + 2ab)^{1/2} + a + b] \qquad (8)$$

If the backscattering cross section were much larger than that for absorption, or $b >> a$, then the equation for a thick cloud becomes

$$\alpha = (2a/b)^{1/2} \qquad (9)$$

For this condition, as the backscattering increases, the energy tends to be reflected back to the free surface which bounds the cloud. The data obtained in this investigation belong to the latter category.

If $a >> b$, the absorptivity predicted in Equation (8) would degenerate to

$$\alpha = 1 - b/(2a) \qquad (10)$$

This situation would occur with a dense cloud of highly absorbent material whose size was much smaller than the wavelength of the incident light.

From the data obtained in this work, absorptivities were computed for various cloud concentrations; the results are plotted in Figures 9, 10, and 11 for various values of nL from 10^6 cm.$^{-2}$ to infinity. The first value would correspond to a cloud 1 cm. in depth whose concentration was 10^6 particles/cc.

The absorptivity of aluminum oxide in carbon tetrachloride was relatively low in the short wavelengths and increased markedly at a wavelength of 6μ, where the absorption cross section was a maximum and the backscattering cross section was low. For this wavelength, the maximum absorptivities of 0.92 and 0.95 were obtained for the smaller and larger particle sizes, respectively. At the longer wavelengths, the absorptivity dropped owing to greater scattering. For the same particle concentration, the absorptivity of the smaller particles was generally lower owing to the larger backscattering cross section relative to the absorption cross section.

The values of absorptivity of the particles in carbon disulfide indicated the same general trend as those for carbon tetrachloride. In the range of wavelengths less than 5μ, the absorptivity was slightly greater for the former suspending medium because of the lower backscattering. For the infinite cloud, a peak absorptivity of 0.95 was obtained. At longer wavelengths, the more concentrated suspensions decreased slightly in absorptivity because of the increased scattering.

A similarity in the general shapes of Figures 9 to 11 was noted. This was primarily due to the fact that in all cases backscattering was predominant for the shorter wavelengths, while absorption was predominant for the longer wavelengths. The region of the maximum ab-

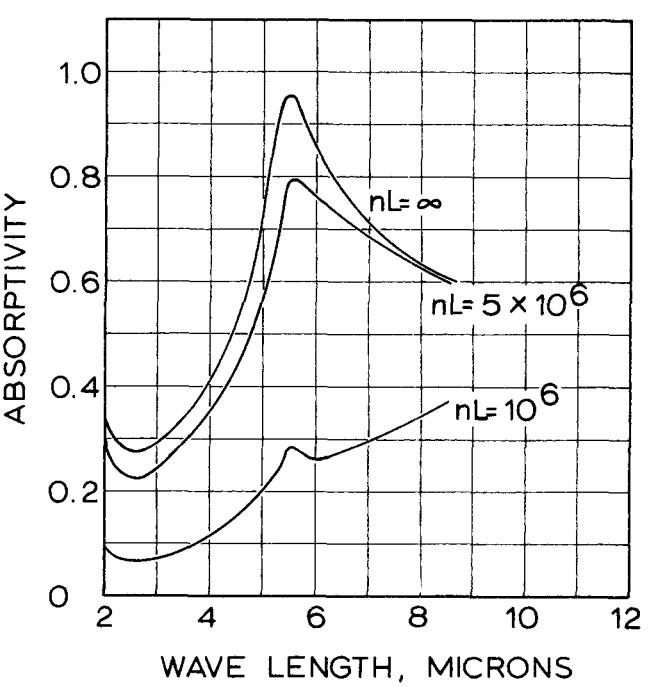

Fig. 11. Absorptivity of a cloud of aluminum oxide particles with a diameter of 12.2μ in carbon disulfide.

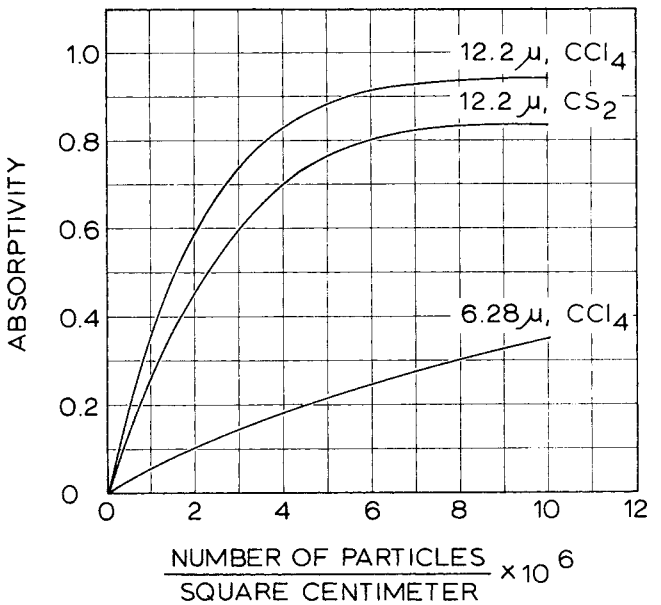

Fig. 12. Absorptivity of various particle clouds for a wavelength of 6.0μ.

sorptivity was in the proximity of 6μ. Where scattering is small, asymptotic values for the infinitely thick clouds approached 0.92 to 0.94. As an illustration of this, Figure 12 was plotted to indicate the variation of absorptivity as a function of the number of particles per square centimeters.

The methods and data presented herein can be used to compute the absorptivities of various particle concentration clouds, provided the same particle material, particle size, and suspending medium are used. Equation (7) can be used with the proper values of a, b, n, and L. The only unknowns in the equations are a and b. These can be obtained from σ_a, σ_e, and B. Interpolation can be used for particles between the sizes investigated.

However, if the computation is made for a different suspending medium, caution should be exercised. Although a generalized correlation obtained for the Mie extinction coefficient proved to be satisfactory for the collimated source, the correlation for the diffuse source has not been completely documented. However, the results of Figure 7 are encouraging. In the absence of experimental data, this correlation might be used with the refractive index to obtain the backscattering coefficient.

CONCLUDING REMARKS

A method has been developed, based upon a two-flux model, which can be used to determine the absorptivity of a cloud of small particles. Limited data are necessary on the transmissivity of various concentrations for prediction. However, a generalized correlation of backscattering coefficient with relative refractive index is suggested which may permit extrapolation to other particle sizes and suspending media. Further experimental data are needed in this area.

NOTATION

a = total absorption cross section, $\alpha_m/n + \sigma_a$, sq.cm.
b = backscattering cross section, sq.cm.
B = backscattering coefficient, $b/(\sigma_e - \sigma_a)$, dimensionless
d = diameter of particle, μ, cm.
i = intensity of forward ray, energy/sterad-μ
j = intensity of backward ray, energy/sterad-μ
L = length of sample cell, cm.
m = parameter, $(a^2 + 2ab)^{1/2}$, cm.
n = population density of cloud, number/cc.
n_p = refractive index of particle, dimensionless
n_m = refractive index of medium, dimensionless
Q_e = Mie extinction coefficient, dimensionless
r = reflectivity of cloud, dimensionless
T = normalized transmission, dimensionless
x = distance of travel of light ray, cm.

Greek Letters

α = absorptivity of cloud, dimensionless
α_m = absorption coefficient of suspending medium, cm.$^{-1}$
λ_0 = wavelength of light in vacuum, μ, cm.
ρ = surface reflectivity, dimensionless
σ_a = absorption cross section, sq.cm.
σ_e = extinction cross section, sq.cm.
ϕ = phase lag, radians

LITERATURE CITED

1. Chandrasekhar, S., "Radiative Transfer," Dover, New York (1960).
2. Kourganoff, V., "Basic Methods in Transfer Problems," Dover, New York (1963).
3. Viskanta R., *Argonne National Laboratory Rept. ANL-6170* (1960).
4. Love, T. J., *Aeronautical Research Laboratories Rept. ARL 63-3* (Jan., 1963).
5. Morizumi, S. J., and H. J. Carpenter, Preprint No. 64-61, Aerospace Sciences Meeting, New York (Jan. 20-22, 1964).
6. Stull, V. R., and G. N. Plass, *J. Opt. Soc. Am.*, **50**, No. 2, 121-129 (Feb., 1960).
7. Mie, G., *Ann. Physik*, **25**, 377 (1908).
8. McAlister, J. A., E. Y. H. Keng, and C. Orr, *NASA CR-325* (Nov., 1965).
9. Schuster, A., *Astrophys J.*, **21**, 1 (1905).
10. Kubelka, P., and F. Munk, *Z. Tech. Physics*, **12**, 593 (1931).
11. Hamaker, H. C., *Phillips Res. Rept.*, **2**, 55, 103 (1947).
12. Larkin, B. K., and S. W. Churchill, *AIChE J.*, **5**, No. 4, 467-474 (Dec., 1959).
13. Chen, J. C., and S. W. Churchill, *ibid.*, **9**, No. 1, 35-41 (Jan., 1963).
14. Lathrop, A. L., *J. Opt. Soc. Am.*, **55**, No. 9, 1097-1104 (Sept., 1965).
15. Churchill, S. W., G. C. Clark, and C. M. Sliepceivch, *Disc. Faraday Soc.*, No. 30, 192-199(1960).
16. Nagy, A. R., Jr., Ph.D. thesis, Univ. So. Calif., Los Angeles (June, 1967).
17. Gumprecht, R. O., and C. M. Sliepcevich, *J. Opt. Soc. Am.*, **57**, No. 1, 90 (Jan., 1953).
18. Van de Hulst, H. C., "Light Scattering by Small Particles," Wiley, New York (1957).
19. Roessler, V. F., and L. Horlacher, *Optik*, **19**, No. 9, 451-462 (Sept., 1962).
20. Gillespie, D. T., A. L. Olesen, and L. W. Nichols, *Appl. Opt.*, **4**, No. 11, 1488-1493 (Nov., 1965).
21. McCarthy, D. E., *ibid.*, No. 3, 317-320 (Mar., 1965).
22. *Ibid.*, **2**, No. 4, 591 (Apr., 1963).
23. Plass, G. N., *ibid.*, **4**, No. 12, 1616-1619 (Dec., 1965).
24. Gryvnak, D. A., and D. E. Burch, *J. Opt. Soc. Am.*, **55**, 625 (1965).
25. Carlson, D. J., C. H. Lewis, R. A. Du Puis, and A. B. Bauer, *Applied Research Laboratories Publication No. U-3044* (Mar. 10, 1965).
26. Hanna, R., *J. Am. Ceram. Soc.*, **4**, No. 7, 376-380 (July, 1965).
27. Lee, D. U., and U. D. Kingery, *ibid.*, **43**, No. 11, 594-607 (Nov., 1960).
28. Florio, J. V., *ibid.*, No. 5, 262-267 (May, 1960).
29. Plass, G. N., *Appl. Opt.*, **5**, No. 2, 279-285 (Feb., 1966).

Manuscript received March 26, 1968; revision received September 3, 1968, paper accepted September 5, 1968.